Source Apportionment and Emission Rates of Volatile Organic Compounds in the Bakken Shale Oil and Natural Gas Region

By

Kati J. VanEtten

Honors Thesis

Appalachian State University

Department of Environmental Science

525 Rivers Street, Boone, NC 28608

Submitted to the Environmental Science Program

and The Honors College

in partial fulfillment of the requirements for the

University Honors and Environmental Science Program Honors

May 2017

APPROVED BY:

_____
Robert F. Swarthout, Ph.D.
Thesis Director

_____
Christopher S. Thaxton, Ph.D.
Environmental Science Program Honors, Director

_____
Christopher S. Thaxton, Ph.D.
Second Reader

_____
Ted Zerucha, Ph.D.
The Honors College, Director

Table of Contents

List of Abbreviations

ONG- Oil and Natural Gas

UONG- Unconventional Oil and Natural Gas

OH- Hydroxyl radical

OHR- Hydroxyl radical reactivity

VOC- Volatile organic compound

OVOC- Oxygenated volatile organic compound

COS- carbonyl sulfide

DMS- dimethyl sulfide

C_2Cl_{4-} tetrachloroethylene

C_2HCl_3- trichloroethylene

n-PrONO_2- n-propyl nitrate

2-BuONO_2- 2-butyl nitrate

3-PenONO_2 3-pentyl nitrate

2-PenONO_2- 2-pentyl nitrate

MeONO_2- methyl nitrate

EtONO_2- Ethyl nitrate

i-$PrONO_2$- *iso*-propyl nitrate

Abstract

Unconventional oil and gas (UONG) production using horizontal drilling and hydraulic fracturing has increased exponentially over the past decade in the Bakken Shale region located in eastern Montana and western North Dakota. Regional air quality is jeopardized during the development of this resource due to the volatile organic compounds (VOCs) that are emitted during drilling, venting and flaring of natural gas, and from leaking oil and gas transportation infrastructure. Limited peer reviewed VOC measurements in the proximity of natural gas fields have been reported despite the environmental and health concerns of the public. In this study, the National Park Service measured VOC mixing ratios during an intensive field campaign in the winter of 2013-2014 to help better understand the potential impacts of these emissions on federal lands. Emission ratios with the tracer compounds, ethyne and propane, derived from a binary mixing model implicate regional oil and natural gas (ONG) production as the source of elevated alkanes in the Bakken Shale when compared to combustion emissions and background mixing ratios. Emission fluxes of alkanes calculated using a mass balance approach were similar to those from other ONG production regions, while annual emission rates for the 28,000 km region were an order of magnitude higher than rates from smaller regions. Hydroxyl radical reactivity was estimated in order to predict future regional ozone production and showed that 20-40% of total hydroxyl radical reactivity was attributable to ONG emissions. These calculations are fundamental to understanding how unconventional ONG production effects regional air quality.

I. Introduction

Unconventional oil and natural gas (UONG) exploration and production in the United States have increased over time due to advances in technology that have contributed to creating an economic climate favoring UONG over conventional energy sources such as coal. Conclusions about UONG trends can be drawn by studying the top four onshore basins in the U.S. that are major contributors to both production and capital expenditure: the Eagle Ford shale, Bakken shale, Permian Basin, and the Marcellus shale. The US EIA reported that the average drilling and completion costs in the four onshore areas decreased by 25% to 30% between their highest point over the past decade in 2012 and 2015 (US EIA, 2016).These areas currently play a large role in UONG production and are predicted to continue impacting the industry in the future.

Although shale oil and gas has been produced in the United States for many decades, it was not considered to be a significant resource until new horizontal drilling and hydraulic fracturing technology facilitated production. Horizontal drilling and hydraulic fracturing were first developed in the 1950's and have been refined over time (Chemical composition of gas, 2016). Technology improvements associated with the completion of the well and key technologies that minimize the material needed for drilling increase the overall performance of drilling (US EIA, 2016). Refinement of well design is expected to continue to progress in the future in order for operators to combat decreasing oil costs and alter drilling strategies to increase efficiency (US EIA, 2016).

Overall, the capital cost decreases and technology advancements have contributed to fluctuating trends in UONG production in the US, and the number of natural gas producing wells (Figure 1). For example, in 2000, oil prices were low at $27/barrel resulting in stagnant

oil field development and little return on investment for current operations (US EIA, 2016). This standstill in oil production quickly rebounded in 2004 with the development of the Barnett Shale that strengthened unconventional onshore drilling. Simultaneously natural gas prices increased resulting in the evolution of other major UONG drilling locations from 2001-2008. Both oil and natural gas prices plummeted in 2008 due to the Global Financial Crisis, also known as the Great Recession. From 2008-2010, oil quickly recovered with continued exploration of productive shale basins using horizontal drilling and hydraulic fracturing. From 2010-2012, the industry expanded at a rate faster than the materials needed could be produced, which halted the pace of well development. Understanding cost drivers and trends are important in predicting future price scenarios. Future well cost trends forecast modest oil recoveries until 2018 due to the overall projected decrease in drilling costs (US EIA, 2016).

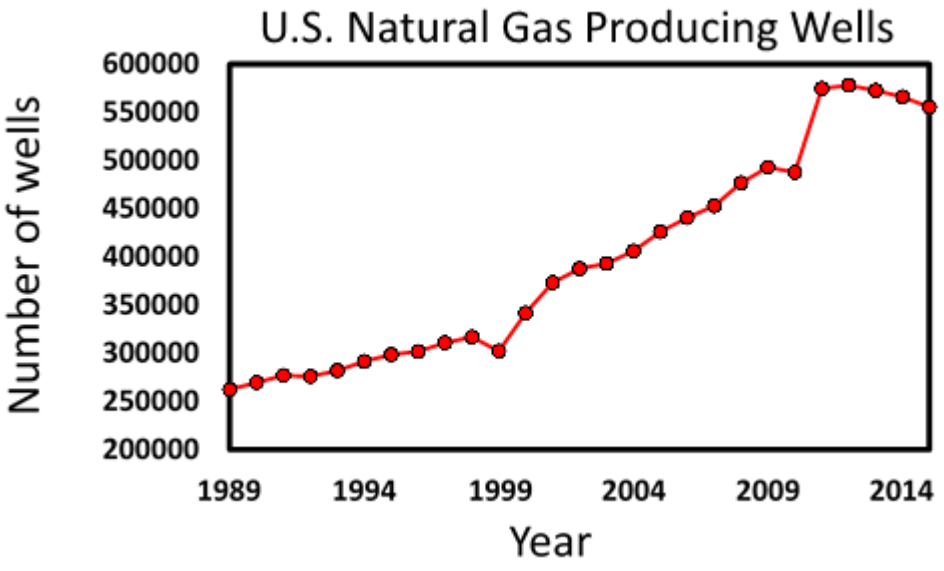

Figure 1: The number of natural gas producing wells has increased from 1989 to 2014.

Geological formations and processes are important when considering the significance of the Bakken Shale to UONG exploration. The Bakken Shale petroleum system encompasses strata from the Devonian Three Forks formation and Bakken formation, and occupies about 200,000 square miles of the subsurface with oil and natural gas reservoirs. The Bakken shale is a rock formation from the Late Devonian (416-358 million years ago) to Early Mississippian age, also known as the Lower Carboniferous period (358-323 million years ago) that is estimated to hold 24 billion barrels of recoverable oil (Prenni et al., 2015). The four members that make up the Bakken formation from oldest to youngest are: the Pronghorn Member, also known as "sanish sand;" the lower shale member; the middle member; and the upper shale member. The Three Forks formation underlies the Pronghorn Member of the Bakken Formation and consists of interbedded greyish green dolomitic mudstones, pink to tan silty dolostones, and anhydrite. It reaches a maximum thickness of 270 feet in the center of the basin, divided by upper and lower units that vary in oil concentrations. The primary source rocks for the Bakken Shale's petroleum consist of the upper and lower shale members which contain black shale and 1-35% by weight of present day total organic carbon (Ked Interests, LLC, 2017). The black shale that was found in the upper and lower shale member of the Bakken formation consists of sand and silt sized particles, known as mud, and deposits of organic matter. Warming and burial of the mud within the earth causes the organic material to break down and may lead to the formation of small ONG reservoirs within shale layers. These small ONG reservoirs also known as drill site "sweet spots," are targeted for UONG exploration and production.

The UONG production process involves a series of steps that are dependent on techniques such as horizontal drilling and hydraulic fracturing. The process begins with

hydrocarbon exploration by petroleum geologists and geophysicists, through visual assessment and survey testing techniques. Areas of geologic interest that are predicted to hold deposits of ONG are then subjected to seismic testing, primarily reflection seismology using vibroseis trucks. Reflection seismology measures the time it takes for reflected sound waves to travel through matter or rock of varying densities, yielding a depth profile of the substructure. Once it is determined that extracting ONG from a specific location is favorable, a well pad is created along with access roads and other facilities. Next, the drilling rig is installed and a drill bore is then driven vertically beneath the ground until it has reach desired depth. In conventional ONG drilling, where large reservoirs of ONG are present, the drilling process would be complete at this point. Unlike conventional drilling, however, unconventional drilling continues from this point to incorporate either horizontal drilling, hydraulic fracturing, or both, to access the small reservoirs of ONG that are typically locked in the impermeable shale. Without horizontal drilling or hydraulic fracturing, shale ONG production would be economically unfeasible because the flow rate of ONG would be so low it would make well development too costly relative to the value of the extracted product.

Horizontal drilling involves repositioning and steering the drill bore horizontal to the subsurface to drill through the shale layer of interest. The drill is then retracted and the loose rock and sediment that is brought to the surface is discarded. A steel casing is placed inside of the well hole, acting as a barrier to nearby aquifers, completing the drilling process. A perforating gun is then used to introduce explosives into the horizontal portion of the well bore to shoot holes through well casing and cement in the deep, horizontal sections of the well to create cracks and fissures, releasing ONG. The drill rig is then replaced with the hydraulic fracturing system.

Hydraulic fracturing increases the permeability of the shale by pumping water and chemicals at high pressures to fracture the shale and liberate the gas from pore spaces. The system pumps water containing proppant (sand), and hydraulic fracturing fluid into the ground at high pressures, once again creating fractures in the rock where ONG can escape. The treatment consists of water-based fluids that are mixed with friction reducing additives (also known as "slickwater"). Other additives include biocides, oxygen scavengers, and acids. The hydraulic fracturing system is then removed and replaced with a production well. Hydrocarbons are pumped to the surface by the production well and the natural gas is flared until production pressure is achieved. Then the well-head is installed, controlling the flow of the product. Equipment that separates oil, gas, water, and other impurities is also installed. The ONG is then stored on site until it is transported to the production facilities by pipeline or tanker truck. Decommissioning of the well takes place when the ONG is depleted in that area. The production and injection wells are closed by removing equipment and debris. Remaining production waste or spill contamination is properly treated and pits and contaminated soils are remediated. Additional topsoil is added and compaction, removal, restoration, and revegetation on sites and roads are necessary.

ONG is formed from mud and organic matter that is compressed and buried over time. Organic matter, such as large quantities of dead organisms including algae and zooplankton from 200-400 mya, are trapped underneath sedimentary layers of the earth and decomposed under intense heat and pressure, forming ONG. ONG consists of varying proportions of oil and natural gas depending on the formation conditions. The elemental composition of crude oil includes carbon and hydrogen composing 83-97% and 10-14%, respectively of the elemental composition of the fluid. Other elements present in the oil include nitrogen (0.1-

2.0%), oxygen (0.1-1.5%), and sulfur (0.5-6.0%) and trace amounts of metals such as iron, nickel, copper, and vanadium (Petroleum Composition, 2013). The hydrocarbons in crude oil include normal, branched, and cyclic alkanes, polycyclic aromatic hydrocarbons resins, and asphaltenes (Petroleum Composition, 2013). The percentages of these hydrocarbons can vary greatly because the characteristics of crude oil are dependent on the source material which varies by geographic region. Natural gas is also a fossil fuel composed primarily of methane (70-100%) with smaller amounts of higher alkanes (0-30%) such as ethane, propane, butane, and pentane and trace amounts of other gasses including benzene (Chemical Composition of Natural Gas, 2013). All of these natural gas constituents are volatile organic compounds (VOCs). Fugitive emissions of VOCs can occur during all stages of the UONG exploration and production process including between transitions of the hydraulic fracturing system, drilling rig, and production rig, as well as from pressurized valves on the well head after production process (Figure 2).

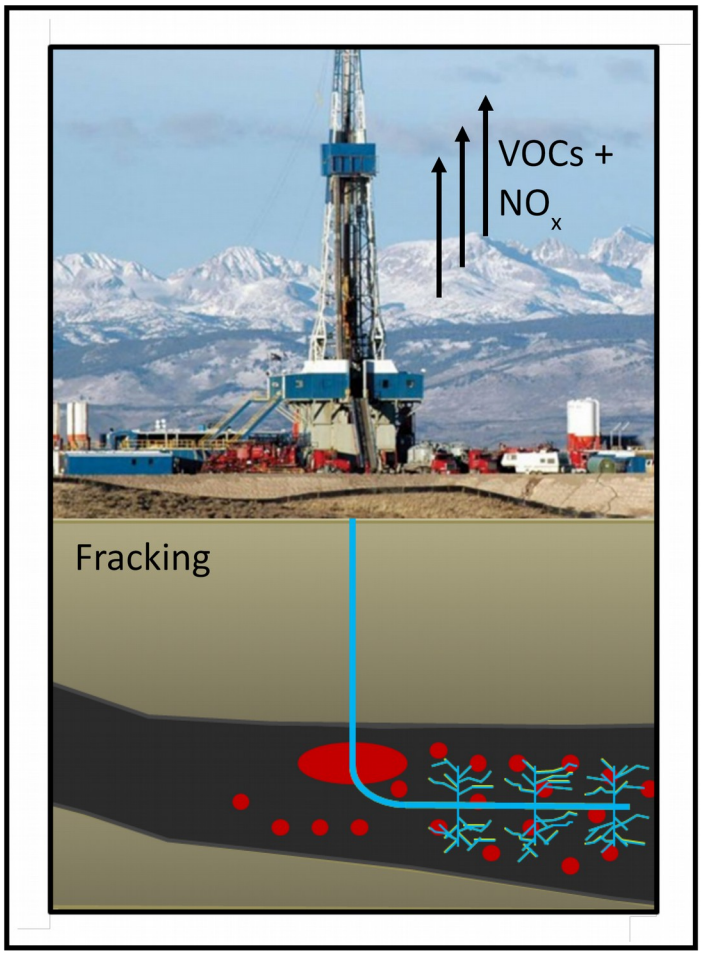

Figure 2: ONG resources are extracted using horizontal drilling and hydraulic fracturing. Volatile organic compounds are emitted during several stages of well development.

VOCs are any compounds that have high enough vapor pressure to exist as a gas at atmospheric pressure and temperature and contain carbon and hydrogen atoms. Different classes of VOCs include hydrocarbons and heteroatomic compounds containing other non-metal elements such as oxygen, nitrogen, and halogens. VOCs encompass a large number of chemicals. For example: alkanes include propane, ethane, i-butane, n-butane, i-pentane, n-pentane, i-hexane; alkenes include ethene and propene; aromatics include benzene, toluene, and the xylenes; oxygenated VOCs (OVOCs) include acetaldehyde and ethanol. These

diverse chemicals have many sources including biogenic, industrial, and combustion emissions. Some VOCs are emitted into the atmosphere from biogenic sources, which include vegetation, microbial metabolism, and soil microorganisms. Industrial VOC sources include household cleaning products such as aerosol sprays, degreasers, and dry cleaning fluids, while combustion VOC sources include vehicle exhaust and biomass burning. VOCs are oxidized in the atmosphere through reaction with the hydroxyl radical (OH) in the presence of sunlight and nitrogen oxides (nitric oxide + nitrogen dioxide = NO + NO_2 = NO_x) to form ozone. High amounts of NO_x exist in large cities where there is a large amount of traffic congestion. NO_x is formed during combustion of fossil fuels when nitrogen and oxygen atoms combine to create NO. This NO further reacts with peroxy radicals (RO_2) to create NO_2. NO_2 can photolyze to yield atomic oxygen which combines with molecular oxygen to form ozone. Exposure to ozone and to some VOCs is associated with negative implications for human health (Webb et al., 2014).

Some VOCs are classified as hazardous air pollutants because they directly impact human health. VOCs such as benzene and acetaldehyde are recognized as carcinogens (Webb et al., 2014). VOCs can also effect human health indirectly when reacting with OH to form alkyl peroxy radicals and initiating ozone formation. Formation of ground-level ozone is also linked to respiratory irritation, heart problems, negative neurological effects, and exacerbation of existing respiratory issues such as asthma and bronchitis (Webb et al., 2014). The level of exposure, length of exposure, and the nature of the volatile organic compound plays a large role on the degree of health impacts observed on humans. Between 2.0 and 2.7 million people each year suffer from exuberated respiratory problems linked to prolonged

exposure to these compounds (Webb et al., 2014). This results in somewhere between $2.5-33.0 billion in health care and early mortality costs (Landrigan, 2015).

Many studies have linked high levels of VOCs to UONG production regions (Webb, 2014). Edwards et al. (2014) measured ozone levels of 120 ppm in the Uintah Basin, Utah, a UONG production region. The wintertime ozone levels in this region spiked in response to the reflection of sunlight from the snow surface and sunny skies, which increased production of OH, and oxidation rates of VOCs emitted from UONG production to RO_2, as well as increasing the rate of NO_2 photolysis to form ozone. Strong temperature inversions trapped the ozone and precursor gases near the ground, exceeded air quality standards set by the Utah Department of Environmental Protection (Edwards et al., 2014).

While studies investigating VOC emissions from ONG production have been conducted on many ONG regions (Edwards et al., 2014), few have investigated ONG impacts on air quality in the Bakken Shale. Concern about potential impacts of poor air quality from emission on federal lands in this region led the National Park Service (NPS) to sponsor the 2013 Bakken Air Quality Study. The investigation and results presented herein were driven by the data obtained in the Bakken Air Quality Study and address the following questions:

1) What are the mixing ratios of VOCs in this region and how do they compare to other ONG production regions?

2) What proportion of the observed VOC mixing ratios can be attributed to ONG emissions?

3) How do VOC emission rates from the Bakken Shale compare to other ONG production regions?

4) What amount of potential ozone production can be attributed to ONG production?

Answering these questions is a critical first step in understanding and mitigating the consequences of UONG production in this region.

II Review of Bakken Air Quality Study Sample Collection and Analysis

A regional measurement campaign was conducted from November 23, 2013 to December 27, 2014 during the winter season within the Bakken Shale. The study region was located within the Williston Basin in eastern Montana and western North Dakota with an active production area of approximately 28,000 km^2. The total number of active ONG wells in this area during 2013 was over 31,000. The NPS collected 289 whole air samples across three sites; Fort Union Trading Center (FOUS), Medicine Lake Montana (MELA), and Theodore Roosevelt National Park (THRO-N) (Figure 3).

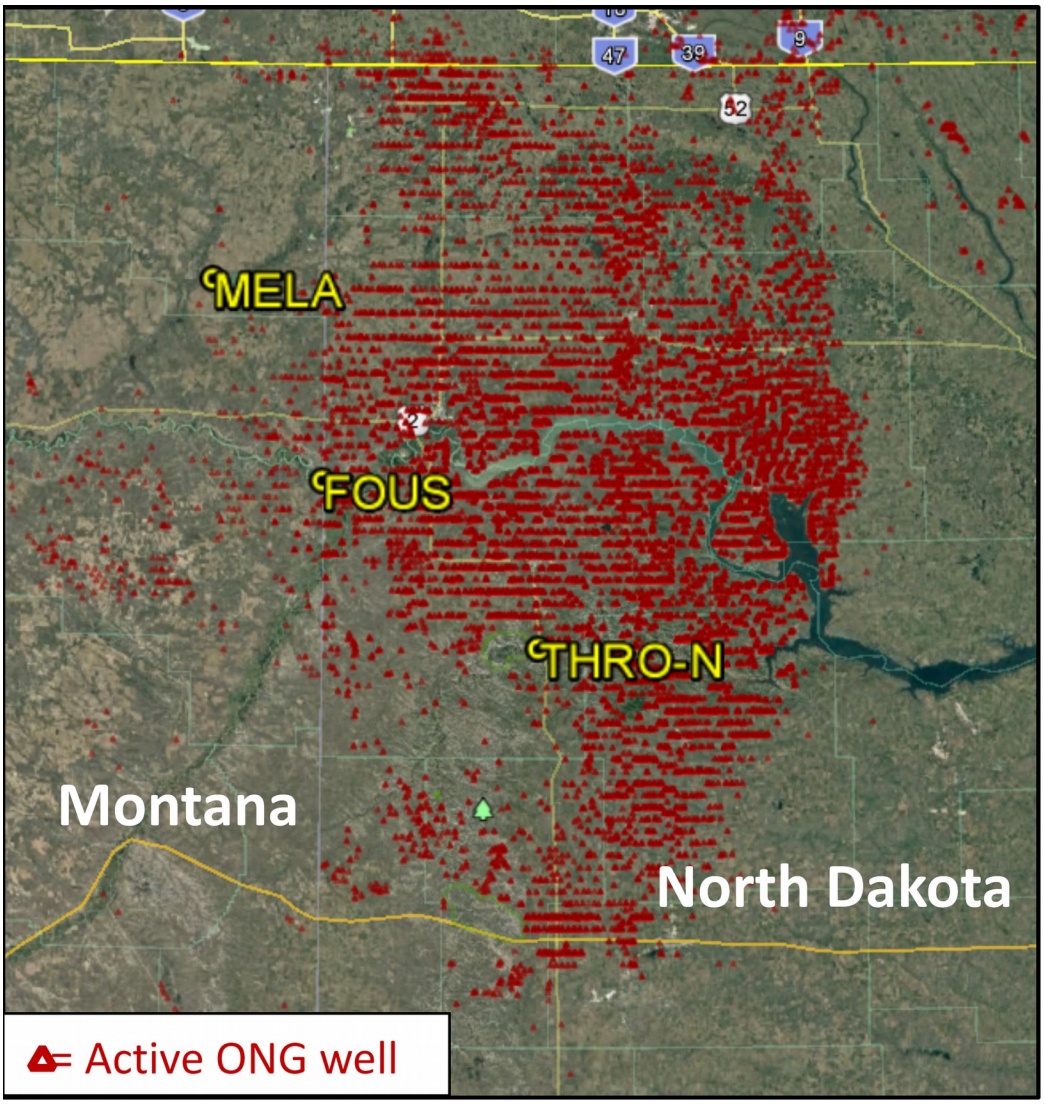

Figure 3: Map of the study region showing the extent of oil and natural gas production. Whole air samples were collected from each of the three sites located on National Park Service lands (yellow circles) surrounded by oil and natural gas wells (red triangles).

The study sites FOUS, MELA, and THRO-N are recognized as three National Park units where FOUS and MELA are located north and to the west of THRO-N. THRO-N is a Class I airshed which provides the highest level of federal protection of its air quality, FOUS is a Class 2 airshed and MELA is a US Fish and Wildlife Class 1 area (Prenni et al., (2016). Major highways that could contribute to potential VOC sources include interstate 94 running

west to east, about 100 km south of THRO-N. Highway 85 runs through the center of ONG activities in the Bakken in McKenzie County, adjacent to THRO-N. Average traffic counts have tripled from 2008-2014, along with increased traffic and increased population to support these activities (Prenni et al., 2016). Other potential VOC sources include coal power plants, landfills, feedlots, and vehicle exhaust.

The samples were collected by NPS staff as part of the Bakken Air Quality Study. Whole air samples were collected in 2 L electropolished stainless steel canisters. Prior to sample collection, each canister was cleaned three times by drawing a vacumm to 10^{-3} Torr, then filling it with ultrahigh purity helium and finally evacuating to a final pressure of 10^{-3} Torr. In the field, evacuated canisters were pressurized to approximately 1400 Torr with ambient air using a metal bellows pump. Samples were collected once every two days in the mid-afternoon time. The study took place in the winter season between November 23, 2013 and March 27, 2014 when 44 samples were collected from FOUS, 18 from MELA, and 227 from THRO-N. The samples were collected in steel canisters at each site.

Samples were then analyzed for VOC mixing ratios by NOAA CIRES (National Oceanic and Atmospheric Administration Corporative Institute for Research in Environmental Science) at Colorado University at Boulder using multi-detector gas chromatography (GC) instrument (figure 4). The VOCs were separated from the air using cryogenic preconcentration system. The VOCs were then channeled through three GCs equipped with five different detectors: two flame ionization detectors (FIDs), two electron capture detectors (ECDs), and a mass spectrometer (Figure 4). Mixing ratios of 49 VOCs (Table 1) were determined using the response factor a calibration curve generated from analysis of National Institute for Standards and Technology (NIST)- traceable standards. This created a rich

dataset of 49 different, measurable VOCs that included alkanes, alkenes, aromatics, and oxygenated volatile organic compounds (OVOCs).

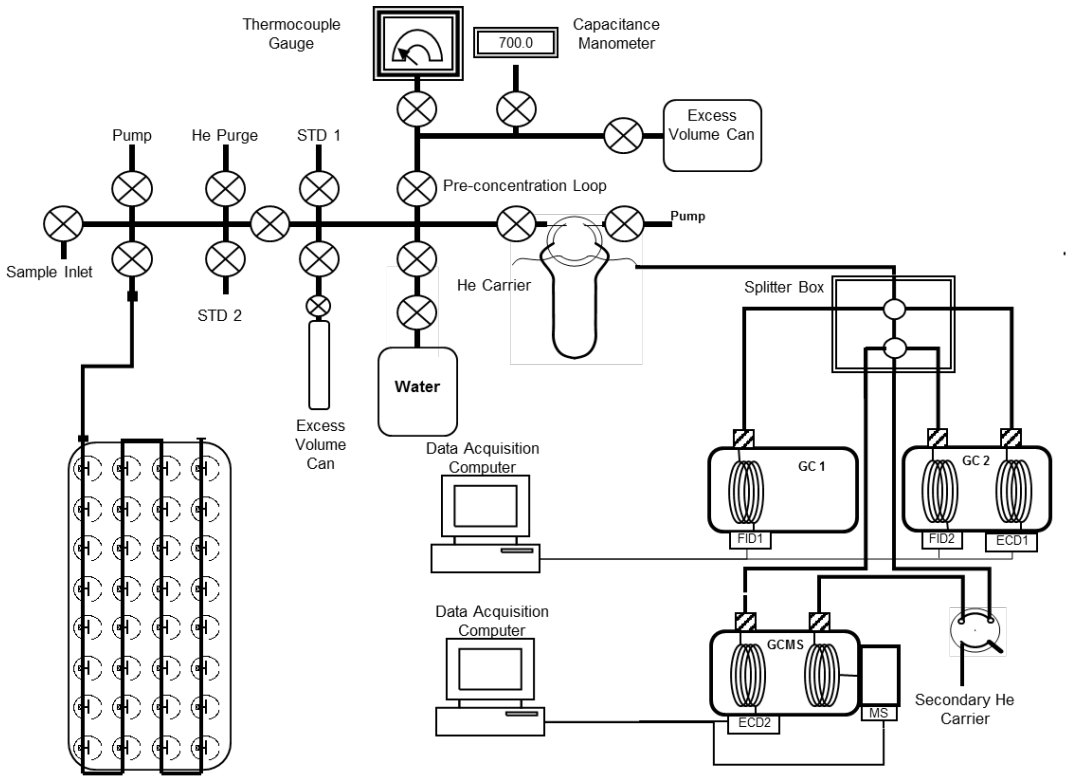

Figure 4: Cryogenic preconcentration separate VOCs from the air. Whole air samples were collected in steel canisters and then delivered to the lab to be separated and analyzed using a multi-detector gas chromatography system, allowing 49 different individual VOCs to be measured.

Source Apportionment

Many of the VOCs measured in this study have numerous emissions sources. Higher alkanes (C_4-C_{10}) and aromatics are emitted from fossil fuel combustion, fuel evaporation, and from leaking ONG infrastructure. Previous studies have suggested that many alkanes and cycloalkanes were most closely associated with ONG sources while aromatics and alkenes were more well correlated with combustion sources (Gilman et al, 2014; Swarthout et al.,

2013; and Swarthout et al., 2015) In addition, these emissions are overlaid on an existing background concentration of each VOC. Therefore, to understand the impacts of ONG emissions on air quality, it is important to determine the extent to which each source contributes to the observed mixing ratios of each VOC.

A binary mixing model based on a multivariate regression was used to account for contributions from ONG and combustion sources, as well as the background mixing ratio of each VOC (Gilman et al., 2013; Swarthout et al., 2015). Furthermore, the proportion of variance not explained by the regression model was classified as "other" unspecified emission sources. The ONG and combustion contributions to a VOC's mixing ratio were determined using the tracer compounds propane and ethyne, respectively. Propane and ethyne are good emissions tracers because they have known sources. Outside of large metropolitan areas, the primary source of propane is ONG production while ethyne is present in any incomplete combustion emissions.

The mixing ratio values of all 49 compounds measured in the 289 whole air mass samples were imported into R-Studio. A separate multivariate regression was conducted for each VOC using the mixing ratios of propane and ethyne as the two dependent variables. The regression solved the following expression (1) for the emission ratio of each compound with the two tracer compounds:

$$[X]_i = bkgd_x + (ER_{propane} \times [propane_{adj}]_i + ER_{ethyne} \times [ethyne_{adj}]_i) \quad (1)$$

The variable $[X]_i$ is the measured mixing ratio of compound X in sample *i*. $Bkgd_x$ is the lowest mixing ratio value of compound X within the entire data set. $Propane_{adj}$ is the difference between the propane mixing ratio in sample *i* and the lowest propane mixing ratio

in the entire data set. Similarly, $ethyne_{adj}$ is the difference between the ethyne mixing ratio in sample *i* and the lowest ethyne mixing ratio in the entire data set. $ER_{propane}$ and ER_{ethyne} are the derived value of the VOC emission ratio of compound X relative to the tracer compound propane and emission ratio of compound X relative to the tracer compound ethyne, respectively. The least squares fit of the model was used to determine both $ER_{propane}$ and ER_{ethyne}. Emission ratios derived from the model were used to characterize the emission source profiles of various VOCs associated with these sources and estimate the relative contribution of each emission source (Gilman et al., 2013). The following equations (2, 3, 4) were used to derive the proportion of each compound attributable to ONG and combustion sources and the background mixing ratio:

$$P_{ONG} = \frac{ER_{propane} \times \mu_p}{ERpropane \times [\mu p] + ERethyne \times [\mu e] + bkgd} \times slope_{model} \quad (2)$$

$$P_{COMB} = \frac{ER_{ethyne} \times \mu_p}{ER\ propane \times [\mu p] + ERethyne \times [\mu e] + bkgd} \times slope_{model} \quad (3)$$

$$P_{BKG} = \frac{ER_{bkg} \times \mu_p}{ER\ propane \times [\mu p] + ERethyne \times [\mu e] + bkgd} \times slope_{model} \quad (4)$$

Where the proportion of ONG (P_{ONG}), combustion (P_{COMB}), and background (P_{BKG}) are the proportion of each VOC mixing ratio that is attributable to ONG sources, combustion sources, and background, respectively, $ER_{propane}$ and ER_{ethyne} are the emission ratios of compound X in respect to propane and ethyne. μ_p and μ_e are the mean mixing ratios of

propane and ethyne for the entire dataset. The numerator in each equation represents the VOC missing ratio attributable to each specific source and the denominator represents the total VOCs mixing ratio observed. $Slope_{model}$ represents the overall slope of the model or the R^2 of the regression. Other sources of emissions that could not be explained by the model were quantified using equation (5):

$$P_{other} = 1 - slope_{model} \quad (5)$$

As the proportion of the variance in the dataset not explained by the multivariate regression model. These other sources include those that are not attributed to any specific source.

Emission Rate Estimate

Estimates of VOC emission rates in ONG production regions provide valuable information to regulators and policy makers. A mass balance approach was used to produce a first-order estimate the rate of emissions produced from ONG sources in the Bakken Shale (Figure 5).

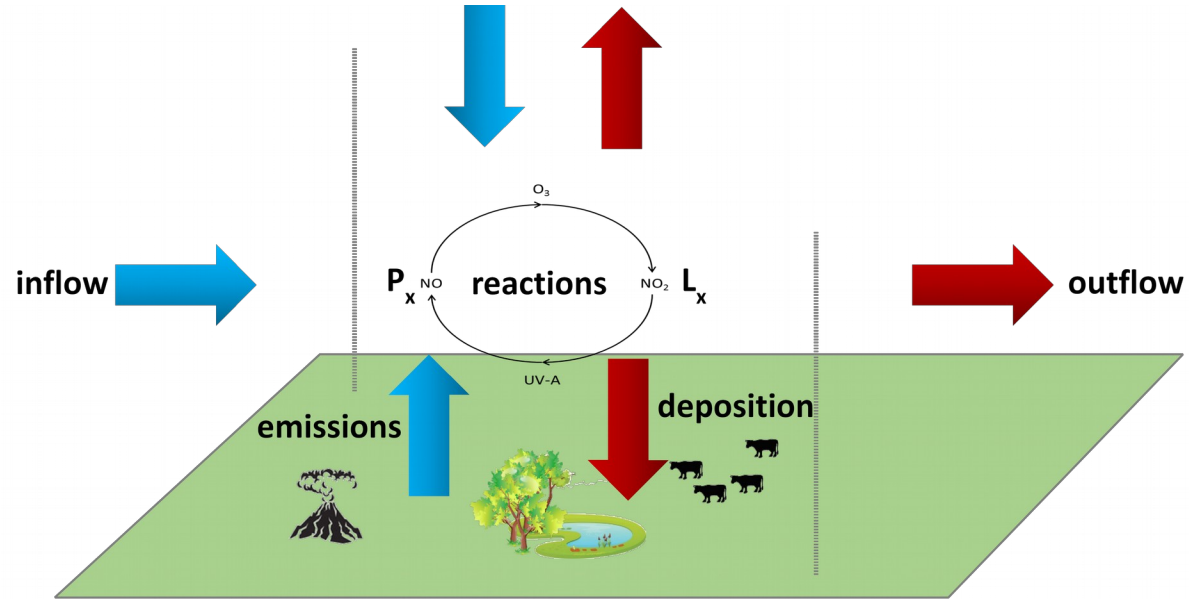

Figure 5: Mass balance model accounts for many fluxes including inflow, outflow, emissions, deposition, and reactions.

The following generalized equation (7) describes the mass balance for any gas in a predetermined area:

$$\frac{\delta C}{\delta t} = +Inflow - Outflow + Production - Removal + Emissions - Deposition \quad (7)$$

where $\delta C/\delta t$ is the change in concentration of compound X over a given amount of time in a designated area, which is a function of the rate of inflow, outflow, production, removal, emissions, and deposition. Many assumptions were made in applying this mass balance approach to the VOC dataset:

1) The system was assumed to be in steady state and the change in the concentration of each compound with respect to time, $\delta C/\delta t$, was assumed to be zero (equation 8) and rearranged to solve for emissions (equation 9).

$$0 = Inflow - Outflow + Production - Removal + Emissions - Deposition \quad (8)$$

$$Emissions = -Inflow + Outflow - Production + Removal + Deposition \quad (9)$$

2) *Production* and *deposition* were assumed to be negligible because the VOCs used in this calculation are not produced by reactions in the atmosphere, and they do not readily deposit to surfaces through dry deposition. The compounds are also sparingly soluble and do not partition into aqueous solutions to be removed through wet deposition in precipitation (equation 10).

$$Emissions = -Inflow + Outflow + Removal \quad (10)$$

3) The difference between the *inflow* and *outflow* concentrations that were attributable to ONG sources was assumed to be the mean concentration of the observed during the study scaled by P_{ONG} determined in the source apportionment. Scaled missing ration were then converted to mass concentrations (g/cm^3) to calculate emissions. This assumption necessarily includes the assumption that measurements from the three study sites were representative of the entire 28,000 km^2 ONG production region (equation 11):

$$Emissions = \frac{\mu_X \times P_{ONG}}{\delta t} + Removal \quad (11)$$

4) In order to calculate an ONG emission rate, δt in equation 11 was estimated as the ventilation time, or the time that it takes the entire air mass in the study region to be replace with a new air mass. A range of ventilation times was estimated according to the following equation (12):

$$Ventilation\ Time = \frac{Fetch}{Wind\ Speed} \quad (12)$$

Where the *fetch* was determined as a function of the wind direction, assumed to be the predominant southwesterly wind direction reported by Prenni et al. (2015) of 225$^{\mathbf{o}}$ ± 18$^{\mathbf{o}}$ and the size of the study area, and the *wind speed* was assumed to be 4.0 ± 2.0 m s^{-1} (Prenni et al., 2015). Using the assumed wind speed and wind direction, and their associated uncertainties, ventilation time was estimated to range between 5.9-10.9 hours (equation 13):

$$Emissions = \frac{\mu_X \times P_{ONG}}{Ventilation\ Time} + Removal \quad (13)$$

5) *Removal* was primarily attributed to reactions of the VOCs with hydroxyl radicals (OH) and the amount of each compound lost to OH oxidation was calculated using published rate constants (Atkinson, 2003; Atkinson et al., 1997, 2006; Atkinson and Arey, 2003), unique to each compound, and assuming the concentration of the hydroxyl radical was a diurnally averaged 1×10^6 molecules/cm^3 (equation 14):

$$Emissions = \frac{\mu_X \times P_{ONG}}{Ventilation\ Time} + k_{OH+X}[OH]\mu_X \qquad (14)$$

6) Finally, to account for the three-dimensional study area, and convert the emission rate to a per unit area emission flux, a boundary layer height (BLH) had to be assumed. The estimated BLH was 550 m ± 200 m based on the analysis of seasonal, diurnal radiosonde data from Saint Louis, Missouri, Salt Lake City, Utah, and Dayton, Ohio conducted by Holzworth (1967). This also includes the assumption that the vertical profile of VOCs in the boundary layer was constant and that the exchange of air between the boundary layer and the free troposphere was negligible (equation 15):

$$Emissions = \left(\frac{\mu_X \times P_{ONG}}{Ventilation\ Time} + k_{OH+X}[OH]\mu_X \right) \times BLH \qquad (15)$$

This emission flux for each VOC was then scaled up to a regional annual emission rate for the 28,000 km^2 Bakken Shale region using the following equation (16):

$$Emission\ Rate = Emission\ Flux \times Area\ of\ Study\ Region \qquad (16)$$

Propagated error calculated for the flux and annual emission rate estimates included the uncertainty of VOC measurements and ventilation time estimates, which included the variability in wind speed and direction and boundary layer height.

Hydroxyl Radical Reactivity

VOCs react with hydroxyl radicals in the presence of nitrogen oxides and sunlight to produce ozone. Determining the kinetic OH reactivity (OHR) of VOC emissions from UNG production serves as a measure for potential ozone production associated with these emissions. High levels of ozone have been shown to have many negative health impacts on humans such as respiratory irritation and negative neurological effects. The rate at which VOCs reacted with hydroxyl radicals was used a proxy to estimate the amount of potential ozone formation in the Bakken Shale Region. The rate of the hydroxyl reaction was calculated by multiplying the concentration of compound X by its hydroxyl radical rate constant (k_{OH+X}), which is unique to each compound (equation 17). The total hydroxyl reactivity is the sum of each individual compound's hydroxyl reactivity (equation 18).

$$OH\ reactivity = k_{OH+Xi}[X]_i \quad (17)$$

$$Total\ OH\ reactivity = \sum k_{OH+Xi}[X]_i \quad (18)$$

Total hydroxyl reactivity was calculated first and then scaled down using the multivariate regression source apportionment model to eliminate contributions from non-ONG sources.

III. Results and Discussion:

Spatial and temporal variability in VOC mixing ratios

The VOC concentrations across FOUS, MELA, and THRO-N had are displayed in table 1a, 1b, and 1c. The mean concentrations of alkanes at MELA were lower than THRON and

FOUS, while the concentration of ethyne and the alkenes and the aromatics were similar across the three sites. Time series of selected VOC mixing ratios including benzene, ethyne, and propane measured during the Bakken Shale study (Figures 6, 7, & 8) relatively similar baseline concentration of each compound with periodic spikes in alkane concentrations as represented by propane in Figure 8.

Table 1a. Mixing ratio (pptv) summary statistics, emission ratios and source apportionment model results for VOCs at Fort Union Trading Post National Historic Site (FOUS).

Compound	Mean	SD	Range	$ER_{propane}$	ER_{ethyne}	ONG (%)	Combust (%)
ethane	17300	18800	2600 - 79900	6.18E-01	1.94E+01	55	30
ethene	5.00E+02	3.00E+02	100 - 1800	3.64E-03	1.10E+00	7	39
propane	1.75E+04	2.62E+04	1800 - 149000	1.00E+00	0.00E+00	95	0
propene	8.00E+01	6.00E+01	20 - 300	4.73E-04	2.03E-01	6	46
trans-2-butene	8.00E+00	5.00E+00	2 - 27	0.00E+00	1.87E-02	0	41
1-butene	2.00E+01	1.00E+01	10 - 50	0.00E+00	4.67E-02	0	62
i-butene	5.00E+01	2.00E+01	20 - 100	0.00E+00	1.15E-01	0	53
cis-2-butene	7.00E+00	5.00E+00	2 - 28	0.00E+00	1.40E-02	0	31
i-butane	2.30E+03	3.40E+03	200 - 19400	1.29E-01	0.00E+00	94	0
n-butane	6.50E+03	1.03E+04	400 - 58100	3.87E-01	0.00E+00	95	0
ethyne	5.00E+02	1.00E+02	300 - 1000	3.31E-18	1.00E+00	0	63
cyclopentane	1.00E+02	1.20E+02	10 - 690	4.55E-03	2.95E-02	78	9
i-pentane	1.30E+03	1.80E+03	200 - 10000	6.74E-02	2.00E-01	87	5
n-pentane	1.50E+03	2.40E+03	100 - 13000	8.83E-02	0.00E+00	93	0
n-hexane	4.00E+02	6.00E+02	<LOD - 3000	2.08E-02	0.00E+00	89	0
n-heptane	1.00E+02	1.50E+02	10 - 760	5.20E-03	3.57E-02	77	9
n-octane	5.00E+01	5.00E+01	<LOD - 250	1.65E-03	6.29E-02	51	34
n-nonane	2.00E+01	1.00E+01	<LOD - 60	3.67E-04	2.58E-02	32	38
benzene	1.00E+02	1.00E+02	100 - 400	2.09E-03	2.33E-01	22	43
toluene	1.00E+02	1.00E+02	<LOD - 200	1.17E-03	1.36E-01	21	43
ethylbenzene	2.00E+01	1.00E+01	10 - 70	2.61E-04	4.18E-02	17	47
m+p-xylene	2.00E+01	2.00E+01	10 - 90	5.13E-04	3.80E-02	30	38
o-xylene	1.00E+01	1.00E+01	<LOD - 30	1.67E-04	1.61E-02	25	42
styrene	2.00E+00	1.00E+00	<LOD - 4	0.00E+00	4.87E-03	0	65
i-propylbenzene	2.00E+00	1.00E+00	1 - 6	1.70E-05	5.22E-03	12	61
n-propylbenzene	3.00E+00	3.00E+00	1 - 15	2.40E-05	7.36E-03	9	48
m-ethyltoluene	5.00E+00	5.00E+00	1 - 19	8.36E-05	1.08E-02	20	44
p-ethyltoluene	3.00E+00	2.00E+00	<LOD - 10	3.05E-05	6.25E-03	15	51
o-ethyltoluene	3.00E+00	2.00E+00	<LOD - 9	2.52E-05	7.16E-03	13	62
1,3,5-trimethylbenzene	3.00E+00	2.00E+00	<LOD - 11	4.32E-05	5.50E-03	22	47
1,2,4-trimethylbenzene	1.00E+01	1.00E+01	<LOD - 40	1.77E-04	1.73E-02	24	40

1,2,3-trimethylbenzene	4.00E+00	3.00E+00	<LOD - 13	4.99E-05	8.16E-03	16	44
1,3-diethylbenzene	1.00E+00	1.00E+00	<LOD - 5	0.00E+00	3.87E-03	0	48
1,4-diethylbenzene	3.00E+00	2.00E+00	1 - 7	0.00E+00	7.30E-03	0	50
1,2-diethylbenzene	2.00E+00	1.00E+00	<LOD - 4	0.00E+00	3.38E-03	0	38
OCS	4.00E+02	1.00E+02	300 - 600	0.00E+00	4.39E-01	0	23
DMS	3.00E+01	2.00E+01	<LOD - 70	0.00E+00	8.07E-02	0	63
C_2HCl_3	2.00E+00	2.00E+00	1 - 9	0.00E+00	5.19E-03	0	35
C_2Cl_4	6.00E+00	2.00E+00	4 - 19	2.21E-05	8.16E-03	4	28
$MeONO_2$	3.40E+00	5.00E-01	2.3 - 5.5	0.00E+00	3.55E-03	0	24
$EtONO_2$	3.00E+00	1.00E+00	1 - 5	0.00E+00	5.84E-03	0	47
i-$PrONO_2$	1.20E+01	5.00E+00	7 - 27	6.64E-05	1.85E-02	8	38
n-$PrONO_2$	2.00E+00	1.00E+00	1 - 3	6.88E-06	3.26E-03	7	57
2-$BuONO_2$	2.00E+01	1.00E+01	<LOD - 60	1.77E-04	4.72E-02	14	65
3-$PenONO_2$	4.00E+00	3.00E+00	<LOD - 16	5.83E-05	1.06E-02	19	59
2-$PenONO_2$	1.00E+01	1.00E+01	<LOD - 30	1.17E-04	2.02E-02	20	59
acetaldehyde (ppbv)	1.00E+00	1.00E+00	<LOD - 4	0.00E+00	3.07E-03	0	39
ethanol (ppbv)	5.00E+00	5.00E+00	1 - 27	1.40E-04	8.48E-03	38	40
acetone (ppbv)	4.00E+00	2.00E+00	1 - 16	0.00E+00	9.77E-03	0	42

Table 1b. Mixing ratio (pptv) summary statistics, emission ratios and source apportionment model results for VOCs at Medicine Lake Site (MELA).

Compound	Mean	SD	Range	$ER_{propane}$	ER_{ethyne}	ONG(%)	Combust(%)
ethane	8.50E+03	1.22E+04	1500 - 47900	1.11E+00	0.00E+00	84	0
ethene	5.00E+02	3.00E+02	100 - 1000	1.07E-02	1.24E+00	10	29
propane	7.10E+03	1.09E+04	800 - 43300	1.00E+00	0.00E+00	90	0
propene	6.00E+01	4.00E+01	20 - 170	1.79E-03	1.54E-01	14	31
trans-2-butene	7.00E+00	2.00E+00	4 - 11	0.00E+00	1.13E-02	0	19
1-butene	1.00E+01	1.00E+01	<LOD - 30	1.51E-04	4.05E-02	6	41
i-butene	5.00E+01	2.00E+01	20 - 70	0.00E+00	1.49E-01	0	46
cis-2-butene	5.00E+00	1.00E+00	3 - 7	0.00E+00	7.70E-03	0	17
i-butane	9.00E+02	1.30E+03	100 - 5200	1.18E-01	2.04E-01	83	4
n-butane	2.40E+03	3.80E+03	300 - 14300	3.37E-01	0.00E+00	89	0
ethyne	4.00E+02	1.00E+02	200 - 500	0.00E+00	1.00E+00	0	43
cyclopentane	4.00E+01	4.00E+01	10 - 190	3.94E-03	2.63E-02	62	10
i-pentane	5.00E+02	7.00E+02	100 - 2700	6.06E-02	2.49E-01	74	8
n-pentane	6.00E+02	8.00E+02	100 - 3200	7.59E-02	0.00E+00	85	0
n-hexane	2.00E+02	2.00E+02	<LOD - 800	1.82E-02	6.79E-02	76	7
n-heptane	5.00E+01	5.00E+01	10 - 200	4.74E-03	3.42E-02	67	12
n-octane	3.00E+01	2.00E+01	10 - 90	1.86E-03	2.46E-02	47	16
n-nonane	1.00E+01	1.00E+01	<LOD - 30	4.95E-04	1.68E-02	35	30
benzene	1.10E+02	4.00E+01	60 - 210	1.84E-03	2.08E-01	10	29
toluene	4.70E+01	2.60E+01	18 - 126	1.90E-03	9.56E-02	25	32
ethylbenzene	1.00E+01	1.00E+01	<LOD - 30	5.14E-04	3.43E-02	22	36
m+p-xylene	1.00E+01	1.00E+01	<LOD - 40	7.23E-04	2.30E-02	34	27
o-xylene	0.00E+00	4.00E+00	2 - 16	2.73E-04	1.23E-02	28	32
styrene	1.00E+00	1.00E+00	<LOD - 3	0.00E+00	4.15E-03	0	30
i-propylbenzene	2.00E+00	1.00E+00	1 - 3	4.17E-05	3.01E-03	13	24
n-propylbenzene	2.00E+00	1.00E+00	<LOD - 5	9.23E-05	5.10E-03	27	37
m-ethyltoluene	3.00E+00	2.00E+00	<LOD - 8	1.40E-04	6.59E-03	32	38
p-ethyltoluene	2.00E+00	1.00E+00	<LOD - 5	1.08E-04	2.72E-03	35	22
o-ethyltoluene	1.00E+00	1.00E+00	<LOD - 4	7.65E-05	4.47E-03	26	38
1,3,5-trimethylbenzene	1.00E+00	1.00E+00	<LOD - 4	6.45E-05	3.79E-03	23	34
1,2,4-trimethylbenzene	5.00E+00	4.00E+00	1 - 15	2.32E-04	9.72E-03	23	24
1,2,3-trimethylbenzene	3.00E+00	2.00E+00	1 - 6	8.02E-05	5.08E-03	16	20
1,3-diethylbenzene	8.00E-01	5.00E-01	0.1 - 1.5	5.93E-05	0.00E+00	39	0
1,4-diethylbenzene	2.00E+00	1.00E+00	1 - 4	6.90E-05	0.00E+00	23	0
1,2-diethylbenzene	8.00E-01	3.00E-01	0.5 - 1.2	0.00E+00	2.92E-03	0	-9

OCS	3.83E+02	4.40E+01	334 - 480	0.00E+00	1.99E-01	0	4
DMS	N/A	N/A	N/A	N/A	N/A	N/A	N/A
C_2HCl_3	2.00E+00	1.00E+00	1 - 7	0.00E+00	5.28E-03	0	18
C_2Cl_4	5.00E+00	1.00E+00	4 - 8	5.73E-05	6.64E-03	6	16
$MeONO_2$	3.40E+00	3.00E-01	2.8 - 3.8	0.00E+00	3.68E-03	0	15
$EtONO_2$	3.00E+00	1.00E+00	2 - 5	0.00E+00	6.11E-03	0	27
i-$PrONO_2$	1.30E+01	5.00E+00	8 - 25	2.42E-04	1.81E-02	10	19
n-$PrONO_2$	2.00E+00	1.00E+00	1 - 3	2.76E-05	3.12E-03	10	29
2-$BuONO_2$	2.00E+01	1.00E+01	10 - 50	6.42E-04	4.04E-02	18	28
3-$PenONO_2$	5.00E+00	4.00E+00	<LOD - 14	2.00E-04	1.59E-02	24	49
2-$PenONO_2$	1.00E+01	1.00E+01	<LOD - 30	4.31E-04	2.82E-02	26	43
acetaldehyde (ppbv)	1.00E+00	1.00E+00	1 - 3	0.00E+00	3.63E-03	0	24
ethanol (ppbv)	4.00E+00	3.00E+00	1 - 11	0.00E+00	1.76E-02	0	42
acetone (ppbv)	1.00E+01	1.00E+01	<LOD - 30	0.00E+00	1.56E-02	0	7

Table 1c. Mixing ratio (pptv) summary statistics, emission ratios and source apportionment model results for VOCs at Theodore Roosevelt National Park (THRO-N).

Compound	Mean	SD	Range	$ER_{propane}$	ER_{ethyne}	ONG (%)	Combust (%)
ethane	1.60E+04	1.71E+04	1500 - 94800	6.87E-01	1.77E+01	57	27
ethene	5.00E+02	3.00E+02	200 - 1400	2.61E-03	1.11E+00	5	41
propane	1.49E+04	2.19E+04	1400 - 164200	1.00E+00	0.00E+00	95	0
propene	7.00E+01	4.00E+01	20 - 230	5.00E-04	1.58E-01	8	45
trans-2-butene	8.00E+00	4.00E+00	3 - 32	0.00E+00	1.84E-02	0	40
1-butene	2.00E+01	1.00E+01	<LOD - 40	0.00E+00	4.66E-02	0	63
i-butene	5.00E+01	2.00E+01	10 - 100	0.00E+00	1.20E-01	0	50
cis-2-butene	6.00E+00	3.00E+00	2 - 26	0.00E+00	1.33E-02	0	32
i-butane	1.90E+03	2.80E+03	100 - 21900	1.27E-01	0.00E+00	93	0
n-butane	5.30E+03	8.40E+03	300 - 64900	3.71E-01	0.00E+00	93	0
ethyne	4.00E+02	1.00E+02	200 - 800	1.16E-18	1.00E+00	0	60
cyclopentane	8.00E+01	1.00E+02	10 - 880	4.14E-03	3.74E-02	68	11
i-pentane	1.10E+03	1.60E+03	100 - 11900	7.00E-02	0.00E+00	88	0
n-pentane	1.30E+03	2.10E+03	100 - 17200	9.13E-02	0.00E+00	87	0
n-hexane	3.00E+02	6.00E+02	<LOD - 5800	2.32E-02	0.00E+00	77	0
n-heptane	1.10E+02	1.90E+02	10 - 2070	6.94E-03	0.00E+00	66	0
n-octane	5.00E+01	7.00E+01	<LOD - 640	2.35E-03	4.89E-02	52	20
n-nonane	2.00E+01	2.00E+01	<LOD - 220	7.91E-04	1.37E-02	47	15
benzene	1.00E+02	1.00E+02	<LOD - 700	1.90E-03	2.36E-01	19	43
toluene	1.00E+02	1.00E+02	<LOD - 600	2.23E-03	8.00E-02	40	26
ethylbenzene	2.00E+01	1.00E+01	<LOD - 120	4.66E-04	2.99E-02	31	36
m+p-xylene	2.00E+01	3.00E+01	<LOD - 300	1.19E-03	1.47E-02	50	11
o-xylene	1.00E+01	1.00E+01	<LOD - 80	3.39E-04	9.44E-03	42	21
styrene	1.00E+00	2.00E+00	<LOD - 11	0.00E+00	4.72E-03	0	34
i-propylbenzene	2.00E+00	1.00E+00	<LOD - 9	1.33E-05	6.46E-03	7	60
n-propylbenzene	3.00E+00	3.00E+00	<LOD - 21	3.81E-05	7.42E-03	11	38
m-ethyltoluene	1.00E+01	1.00E+01	<LOD - 60	1.43E-04	9.18E-03	22	25
p-ethyltoluene	3.00E+00	4.00E+00	<LOD - 33	4.21E-05	7.03E-03	9	28
o-ethyltoluene	3.00E+00	3.00E+00	<LOD - 27	3.42E-05	7.43E-03	10	37
1,3,5-trimethylbenzene	3.00E+00	5.00E+00	<LOD - 43	9.47E-05	5.38E-03	19	19
1,2,4-trimethylbenzene	1.00E+01	2.00E+01	<LOD - 160	2.82E-04	1.81E-02	18	20
1,2,3-trimethylbenzene	0.00E+00	1.00E+01	<LOD - 50	4.59E-05	1.17E-02	7	30
1,3-diethylbenzene	2.00E+00	3.00E+00	<LOD - 23	0.00E+00	5.99E-03	0	21
1,4-diethylbenzene	0.00E+00	1.00E+01	<LOD - 50	0.00E+00	1.12E-02	0	20
1,2-diethylbenzene	2.00E+00	2.00E+00	<LOD - 16	0.00E+00	4.65E-03	0	22
OCS	4.00E+02	1.00E+02	200 - 600	0.00E+00	4.82E-01	0	25
DMS	1.00E+01	1.00E+01	<LOD - 30	0.00E+00	4.18E-02	0	39
C_2HCl_3	2.00E+00	1.00E+00	<LOD - 14	1.00E-05	5.51E-03	5	46
C_2Cl_4	5.00E+00	2.00E+00	3 - 21	4.74E-05	7.42E-03	11	30
$MeONO_2$	3.30E+00	4.00E-01	2.2 - 4.4	0.00E+00	3.88E-03	0	24
$EtONO_2$	3.00E+00	1.00E+00	1 - 6	0.00E+00	6.37E-03	0	47
i-$PrONO_2$	1.20E+01	5.00E+00	6 - 44	3.28E-05	2.18E-02	3	34
n-$PrONO_2$	1.00E+00	1.00E+00	<LOD - 6	0.00E+00	3.88E-03	0	55
2-$BuONO_2$	2.00E+01	1.00E+01	<LOD - 90	6.66E-05	5.68E-02	4	64
3-$PenONO_2$	4.00E+00	3.00E+00	<LOD - 23	1.93E-05	1.22E-02	5	55
2-$PenONO_2$	1.00E+01	1.00E+01	<LOD - 50	3.81E-05	2.39E-02	5	56
acetaldehyde (ppbv)	2.00E+00	1.00E+00	<LOD - 11	0.00E+00	4.53E-03	0	31
ethanol (ppbv)	5.00E+00	4.00E+00	<LOD - 21	8.79E-05	1.13E-02	17	40
acetone (ppbv)	4.00E+00	2.00E+00	1 - 14	0.00E+00	1.03E-02	0	43

Table 2: Summary Statistics of VOC Mixing Ratios and OH Reactivities for All Sites

	Mixing Ratio (pptv)				OH Reactivity (s^{-1})	
Compound	**Mean**	**SD**	**Range**	**Median**	**Mean**	**SD**
ethane	1.73E+04	1.72E+04	1500 - 94800	8800	0.097	0.106
ethene	5.00E+02	3.00E+02	100 - 1800	400	0.111	0.060
propane	1.75E+04	2.22E+04	800 - 164200	6900	0.401	0.602
propene	8.00E+01	4.00E+01	20 - 300	60	0.052	0.031
t-2-butene	8.00E+00	4.00E+00	<LOD - 30	10	0.000	0.000
1-butene	2.00E+01	1.00E+01	<LOD - 50	10	0.012	<0.01
i-butene	5.00E+01	2.00E+01	10 - 100	50	0.057	0.027
c-2-butene	7.00E+00	4.00E+00	<LOD - 30	10	<0.01	<0.01
i-butane	2.30E+03	2.90E+03	100 - 21900	900	0.099	0.149
n-butane	6.50E+03	8.50E+03	300 - 64900	2300	0.301	0.483
ethyne	5.00E+02	1.00E+02	200 - 1000	400	0.011	<0.01
cyclopentane	1.00E+02	1.00E+02	10 - 880	40	<0.01	<0.01
i-pentane	1.30E+03	1.60E+03	100 - 11900	500	0.096	0.140
n-pentane	1.50E+03	2.10E+03	100 - 17200	600	0.122	0.199
n-hexane	4.00E+02	6.00E+02	<LOD - 5800	200	0.044	0.072
n-heptane	1.00E+02	1.80E+02	10 - 2070	50	0.017	0.030
n-octane	5.00E+01	6.00E+01	<LOD - 640	30	<0.01	0.013
n-nonane	2.00E+01	2.00E+01	<LOD - 220	10	<0.01	<0.01
benzene	1.00E+02	1.00E+02	<LOD - 700	100	<0.01	<0.01
toluene	1.00E+02	1.00E+02	<LOD - 600	100	<0.01	<0.01
ethylbenzene	2.00E+01	1.00E+01	<LOD - 120	10	<0.01	<0.01
m+p-xylene	2.00E+01	3.00E+01	<LOD - 300	10	0.011	0.015
o-xylene	1.00E+01	1.00E+01	<LOD - 80	10	<0.01	<0.01
styrene	2.00E+00	2.00E+00	<LOD - 10	<LOD	<0.01	<0.01
i-propylbenzene	2.00E+00	1.00E+00	<LOD - 10	<LOD	<0.01	<0.01
n-propylbenzene	3.00E+00	3.00E+00	<LOD - 20	<LOD	<0.01	<0.01
3-ethyltoluene	5.00E+00	6.00E+00	<LOD - 60	<LOD	<0.01	<0.01
4-ethyltoluene	3.00E+00	3.00E+00	<LOD - 30	<LOD	<0.01	<0.01
2-ethyltoluene	3.00E+00	3.00E+00	<LOD - 30	<LOD	<0.01	<0.01
1,3,5-trimethylbenzene	3.00E+00	4.00E+00	<LOD - 40	<LOD	<0.01	<0.01
1,2,4-trimethylbenzene	1.00E+01	1.00E+01	<LOD - 160	10	<0.01	0.011
1,2,3-trimethylbenzene	4.00E+00	5.00E+00	<LOD - 50	<LOD	<0.01	<0.01
1,3-diethylbenzene	1.00E+00	3.00E+00	<LOD - 20	<LOD	<0.01	<0.01
1,4-diethylbenzene	3.00E+00	5.00E+00	<LOD - 50	<LOD	<0.01	<0.01
1,2-diethylbenzene	2.00E+00	2.00E+00	<LOD - 20	<LOD	<0.01	<0.01
OCS	4.00E+02	1.00E+02	200 - 600	400	<0.01	<0.01
DMS	3.00E+01	2.00E+01	<LOD - 70	10	<0.01	<0.01
C2HCl3	2.00E+00	1.00E+00	<LOD - 10	<LOD	<0.01	<0.01
C2Cl4	6.00E+00	2.00E+00	<LOD - 20	<LOD	<0.01	<0.01
MeONO2	3.40E+00	4.00E-01	<LOD - 10	<LOD	<0.01	<0.01
EtONO2	3.00E+00	1.00E+00	<LOD - 10	<LOD	<0.01	<0.01
i-PrONO2	1.20E+01	5.00E+00	10 - 40	10	<0.01	<0.01
n-PrONO2	2.00E+00	1.00E+00	<LOD - 10	<LOD	<0.01	<0.01
2-BuONO2	2.00E+01	1.00E+01	<LOD - 90	20	<0.01	<0.01
3-PenONO2	4.00E+00	3.00E+00	<LOD - 20	<LOD	0.000	0.000
2-PenONO2	1.00E+01	1.00E+01	<LOD - 50	10	0.000	0.000
acetaldehyde (ppbv)	1.00E+00	1.00E+00	<LOD - 10	<LOD	0.582	0.489
ethanol (ppbv)	5.00E+00	4.00E+00	<LOD - 30	<LOD	0.434	0.385
acetone (ppbv)	4.00E+00	3.00E+00	<LOD - 30	<LOD	0.013	<0.01

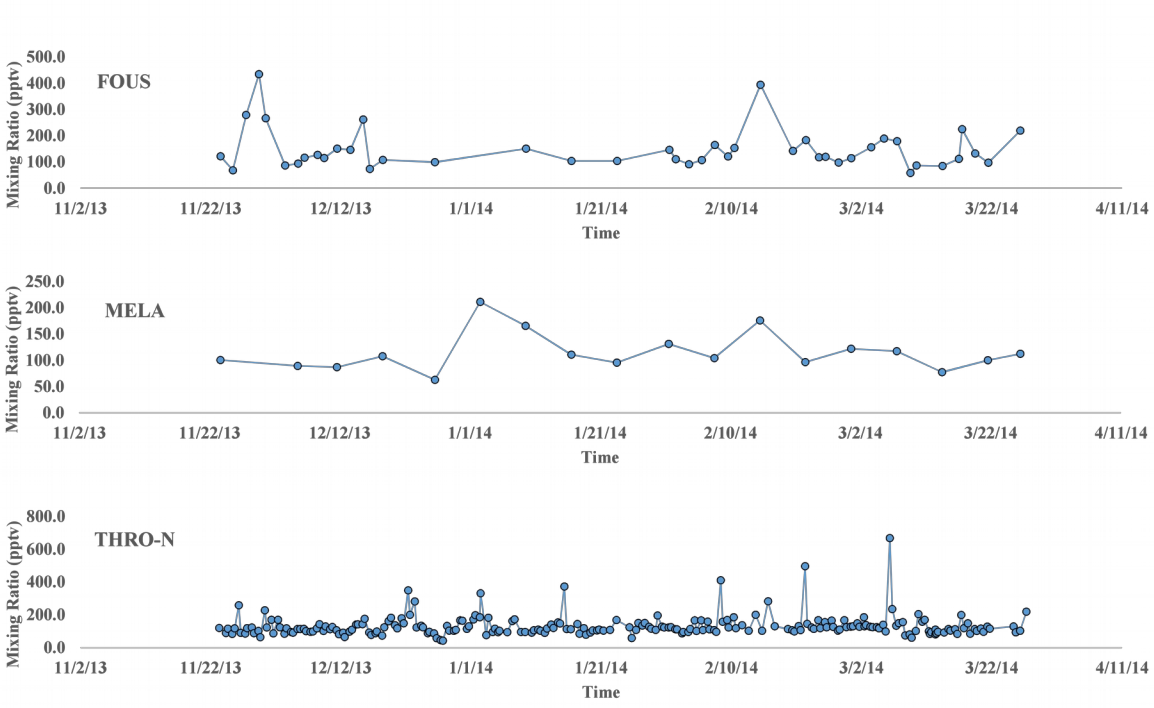

Figure 6: Time series plots of the VOC benzene at each of the three sites, FOUS (top), MELA (middle) and THRON-N (bottom), from 11/23/2013 to 3/26/2014.

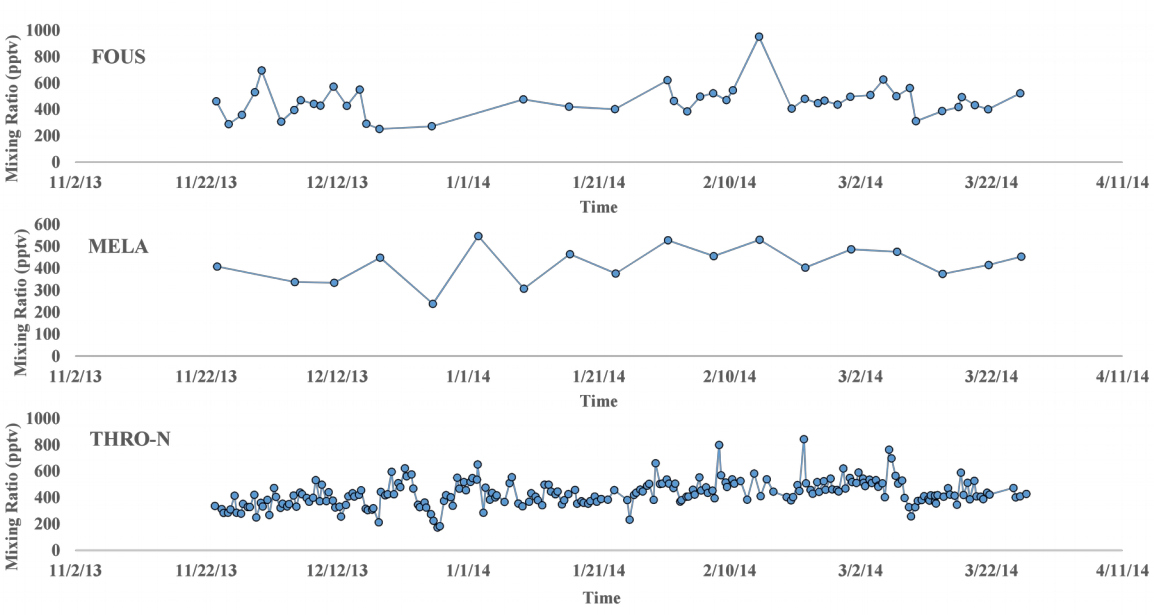

Figure 7: Time series plots of the VOC ethyne at each of the three sites, FOUS (top), MELA (middle) and THRON-N (bottom), from 11/23/2013 to 3/26/2014.

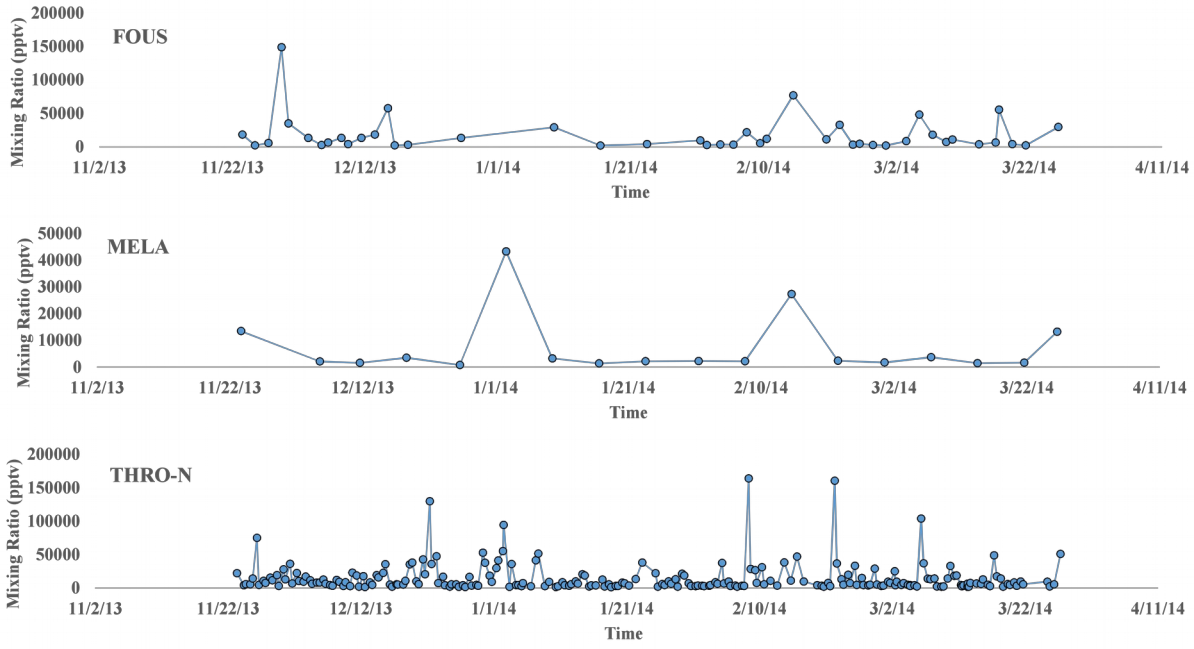

Figure 8: Time series plots of the VOC propane at each of the three sites, FOUS (top), MELA (middle) and THRON-N (bottom), from 11/23/2013 to 3/26/2014.

The mixing ratios of all 49 VOCs were examined across all three locations using a box and whiskers plot (Figure 9). Also shown are average mixing ratios in other UONG sites for comparison. The box and whiskers plots show the mean of the VOC mixing ratios, which is the dotted line, the median, which is the black line, the interquartile range, which is the grey box, and the 5th and 95th percentiles, which are the extent of the whiskers. Measurements from other polluted sites are represented by different symbols: yellow diamonds are the mean mixing ratios reported for the Julesburg-Basin in Northeast Colorado (Swarthout et al., 2013); red triangles are the range of mean mixing ratios reported for 28 U.S. cities measured during summer between 1999 and 2005 (Baker et al., 2008); pink circles are the mean mixing ratios in Houston ship channel/ Galveston Bay, August-September 2006 (Gilman et al., 2009); lime green boxes are the 24 h mean mixing ratio in Mexico City (Apel et al., 2010);

blue triangles are the mean mixing ratios in SW U.S. during September 2001 and April 2002 (Katzenstein et al. 2003); blue stars are the mean mixing ratios reported for the Marcellus Shale UNG development in Southwest Pennsylvania (Swarthout et al., 2015).

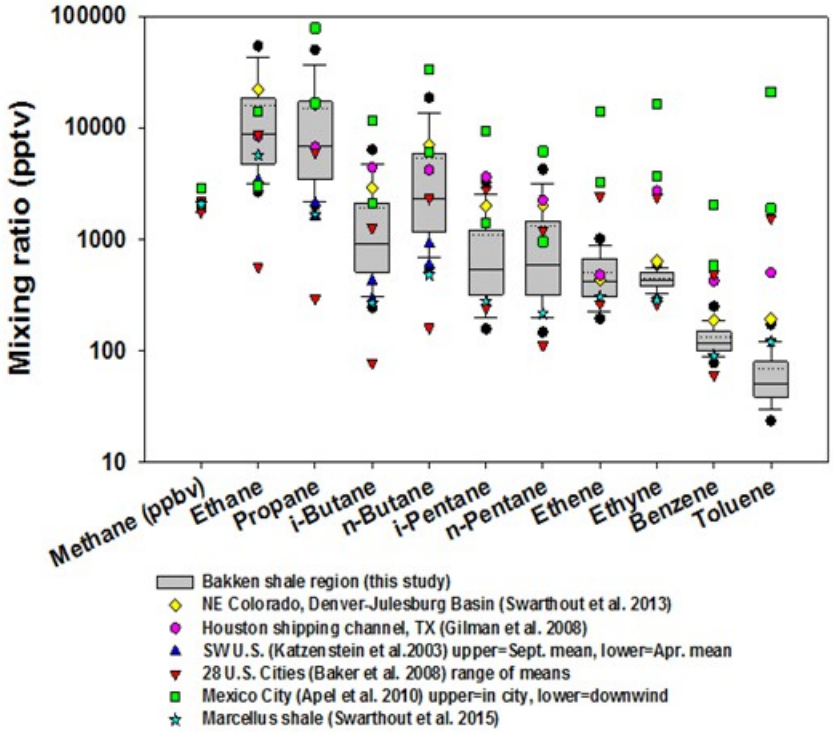

Figure 9: Mixing ratios ov selected VOCs measured in the Bakken Shale compared to measurements from other ONG production areas and polluted sites.

The Bakken Shale VOC mixing ratios generally fall in the range between those in Denver-Julesburg Basin, Colorado, and the Marcellus Shale; lower than the Denver-Julesburg Basin and slightly higher than the Marcellus Shale values. Measurements from Mexico City were higher, which is to be expected as Mexico City is one of the largest megacities in the world. Overall, the Bakken Shale had high VOC mixing ratios similarly to other locations with poor air quality.

Source Apportionment

The predominant source for the alkanes was ONG production, represented in blue in the 100% stacked graph shown in Figure 10. Between 67 and 93% of these gases came from ONG sources. Alkenes were more related to combustion sources and other sources not explained by the model. The aromatics showed a more even distribution of sources with only 12 to 30% of these gases coming from ONG sources. This approach allowed the ONG sources to be separated from all other emission sources that do not emit appreciable amounts of propane including power plants, feedlots, landfills, and vehicle exhaust. Knowing how much of each of these compounds is coming from ONG sources allows for the calculation of emissions and impacts that are directly related to ONG production.

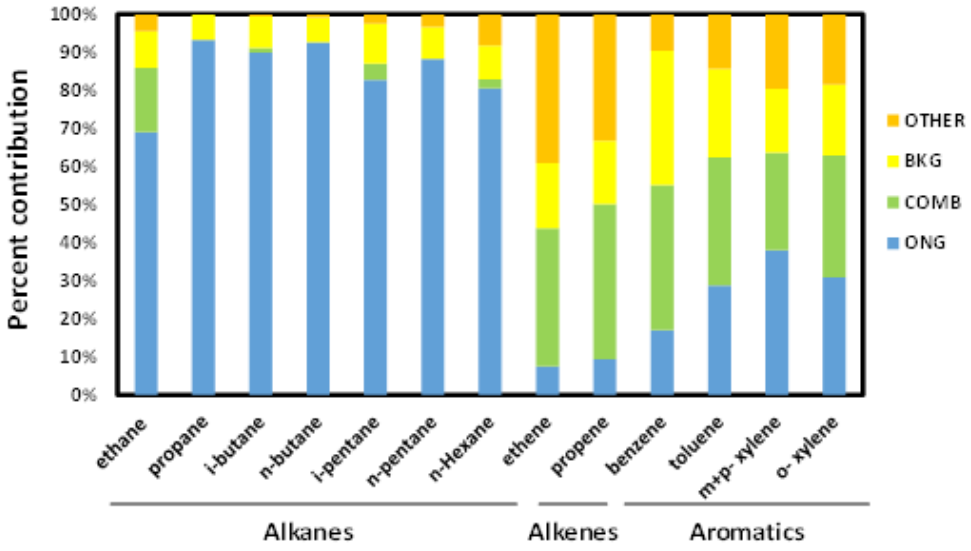

Figure 10: Apportionment of VOC mixing ratios between ONG, combustion, background, and other sources.

Emission Fluxes and Annual Emission Rates

Emission fluxes in the Bakken Shale results included 0.0056±.005 Gg/km^2/yr ethane, 0.0097 ±0 .0090 Gg/km^2/yr propane, 0.0016± 0.0010 Gg/km^2/yr i-butane, 0.0048±0.0040 Gg/km^2/yr n-butane, 0.0011± 0.0009 Gg/km^2/yr i-pentane, 0.0014±0.0010 Gg/km^2/yr n-pentane, and 0.0004 ± 0.0003 Gg/km^2/yr n-hexane (Figure 11). Swarthout et al. (2013) conducted a three-week intensive measurement campaign at the National Oceanic Atmospheric Administration (NOAA) Boulder Atmospheric Observatory (BAO) tower. Whole air mixing ratio air measurements were collected over five nights in February 2011 for several alkanes and benzene at the NOAA BAO tower site located in the Wattenberg Field within Weld County, CO on the southwest edge of the Denver-Julesburg Basin. Propane emission fluxes were 0.0051 ± 0.0012 Gg/km^2/yr for the Wattenberg Field area and 0.0039 ± 0.0055 Gg/km^2/yr for Weld County. Petron et al., 2012 also conducted a study in Weld County in 2008 to bring new independent constraints for the estimation of venting and flashing emissions which measured propane fluxes 0.0034 ± 0.0085 Gg/km^2/yr.

When comparing flux observations of ethane and propane, the Bakken Shale region was higher than reported by previous studies in Colorado. Estimates of other flux measurements of i-butate, n-butane, i-pentane, n-pentane, and n-hexane were similar to those reported by multiple studies in Colorado. One of the reasons that propane and ethane fluxes may be greater in the Bakken Shale is because, unlike other locations, much of the ONG produced in this region is flared instead of collected due to a lack of natural gas pipeline infrastructure in the region. When observing estimated emission rates, possible sources that may have caused higher values to be reported from this study in comparison to those of Swarthout et al. (2013) and Petron et al.(2012) are listed below;

- Regional differences in number of wells and common production practices such as flaring of gas in Bakken whereas other areas collect gas.
- Seasonal differences in temperature may play a role in emissions of VOCs from pressure relief valves and pneumatic valves on well heads.
- Differences in assumed spatial and temporal homogeneity of measurements such as assuming a constant vertical profile throughout the larger boundary layer height (BLH) in this study while other studies assume lower BLH. Assuming measurements from few sites are regionally representative or that measurements from few time points are representative of the entire year may have also effected emission rate calculation.

It is important to note that this estimate should be considered a first-order, preliminary value was used to solve emission flux and rate values (Figure 11) which involved a high degree of uncertainty and relied on many assumptions; however, it is one of the first empirically-based estimates of emissions from this important, but understudied ONG region. Emission fluxes from ONG sources in the Bakken Shale calculated using a mass balance approach compared to other ONG regions in Colorado and Pennsylvania (Figure 11). Annual emission rate from ONG sources in the Bakken Shale, calculated using a mass balance approach, are compared to other ONG regions in Colorado and Pennsylvania (Figure 12).

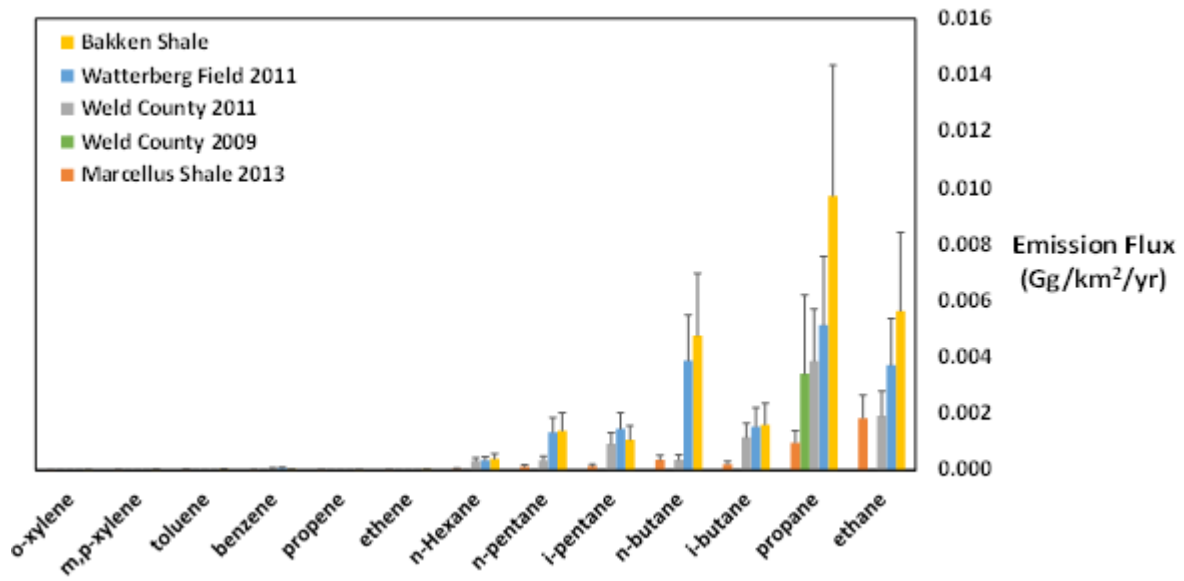

Figure 11: Emission fluxes (Gg/km^2/yr) for a subset of VOCs for the Bakken shale (yellow), Watterberg field (blue), Weld County (gray), Weld County 2009 (green), and Marcellus Shale (orange). Error bars represent propagated uncertainty.

Total annual emission rate in the Bakken Shale were calculated by scaling up the flux estimates by the total area of the heavily drilled portion of the study area (28,000 km^2) and included 265 ± 156 Gg/yr ethane, 45000 ± 259 Gg/yr propane, 74.2 ± 42 Gg/yr i-butane, 219 ± 123 Gg/yr n-butane, 49.1 ± 27 Gg/yr i-pentane, 63.6 ± 35 Gg/yr n-pentane, 18.3 ± 10 Gg/yr n-hexane (Figure 12). Swarthout et al. (2013) extrapolated propane emissions were 13 ± 3 Gg yr^{-1} for the Wattenberg Field area and 40 ± 4 Gg yr^{-1} for Weld County. Petron et al. (2012) estimated propane fluxes ranged from 21.5-64.8 Gg/yr, with a best estimate of 35.7 Gg/yr. Assuming that measurements from the three Bakken Shale sites were representative of year-round emission from the entire heavily drilled region, emissions from the Bakken Shale were an order of magnitude higher than previous estimates from Colorado and Pennsylvania, due primarily to the larger area covered by a high spatial density of UONG wells.

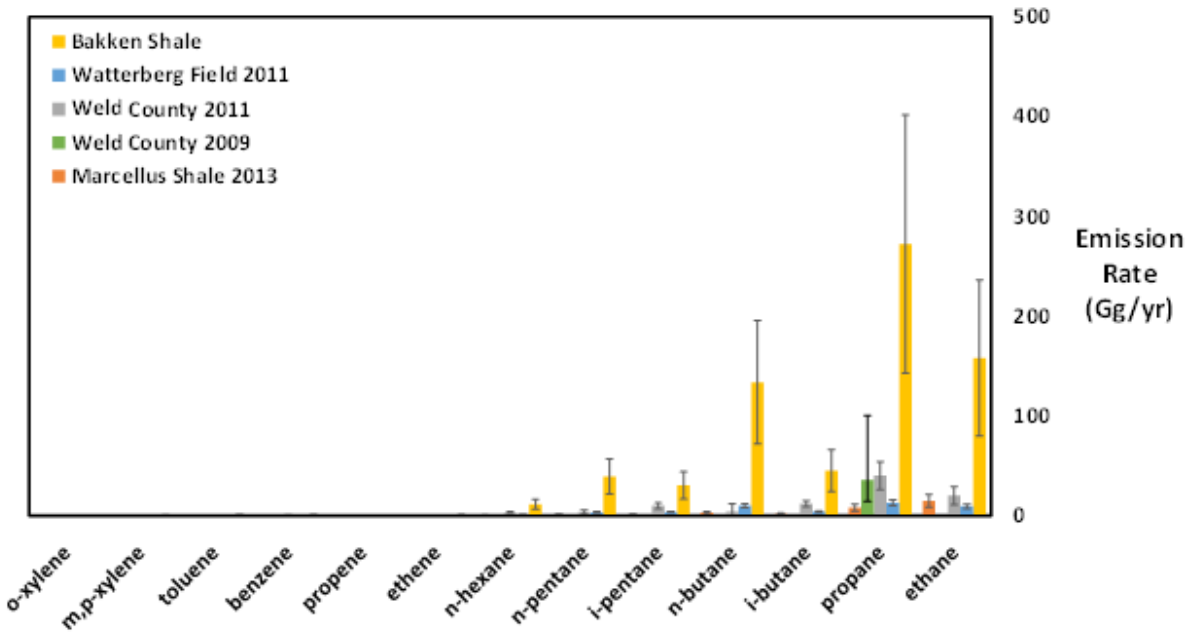

Figure 12: Emission rate (Gg/yr) for selected VOCs for the Bakken shale (yellow), Watterberg field (blue), Weld County 2011(gray), Weld County 2009 (green), and Marcellus Shale (orange). Error bars represent propagated uncertainty.

Hydroxyl Reactivity and Potential Ozone Production

VOCs react with hydroxyl radicals (OH), at well-known rates, to eventually produce hydroperoxy radicals (HO_2) or alkyl peroxy radicals (RO_2). These peroxy radicals oxidize nitric oxide (NO) to nitrogen dioxide (NO_2) and, in the presence of sunlight, NO_2 photolyzes to produce NO and atomic oxygen (O). The atomic O produced in this manner rapidly combines with molecular oxygen (O_2) to produce ozone (O_3). Therefore, determining the rate of the first step in this radical chemical sequence, or the rate of reaction between OH and any VOC emissions from UONG production, serves as a measure of potential ozone production associated with these emissions. This quantity is termed *kinetic OH reactivity* (OHR) and can

provide information on the greatest potential sources of O_3 for determining regulatory targets for O_3 reduction.

Total OHR of all measured VOCs and OVOCs is shown on the left of Figure 10, broken down by compound class. The total OHR was dominated by a mix of alkanes and OVOCs with alkenes making up a smaller proportion. The multivariate regression source apportionment model was used to scale down the total OHR to OHR specifically attributed due to ONG emissions on the right of Figure 10. The vast majority of the ONG associated with OHR is due to alkane emissions and ONG emissions make up approximately 20-40% of the total OHR at the three sampling sites, with the greatest ONG contribution at THRO-N and lesser contributions at FOUS and MELA. The estimate that ONG emissions made up 20-40% of total OHR was due to the large amount of reactive VOCs that are emitted through ONG processes when compared to combustion processes. Alkanes were the largest contributor to ONG OHR at all three sites, indicating that emissions of raw, unprocessed natural gas were primarily responsible for the observed ONG OHR. Raw natural gas containing higher proportions of C_2-C_6 alkanes relative to processed natural gas, which is nearly 100% methane, can be emitted from several steps in the ONG production process such as drilling, venting and flaring of natural gas, and from leaking oil and gas transportation infrastructure. The large percentage of OHR attributed to ONG emissions could lead to increased ozone mixing ratios in downwind cities where there is abundant NO and NO_2 (NO_x). This could have negative implications for human health in these areas as well as being an economic concern for cities struggling to comply with air quality regulations.

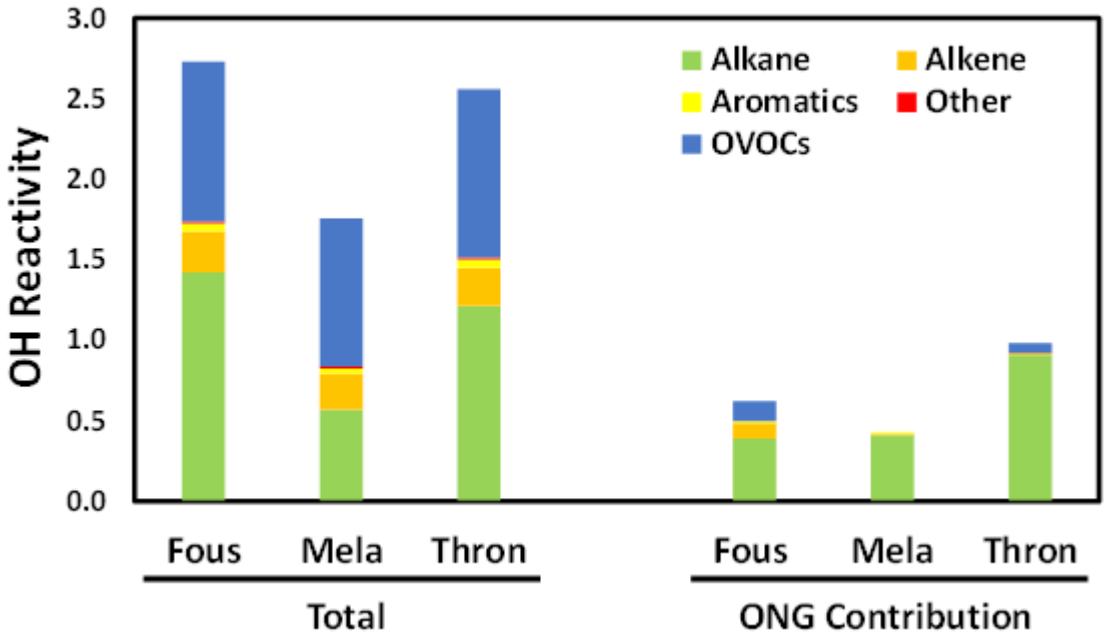

Figure 13: Total and ONG associated hydroxyl radical (OH) reactivity of all measured VOCs and OVOCs. Contributions of ONG emissions are the total OH reactivity scaled by the proportion of mixing ratios attributed to ONG sources in the multivariate regression source apportionment model. Green represents alkane gasses, yellow represents aromatic gasses, blue represents OVOCs, orange represents alkenes, and red represents other gasses that cannot be explained by the model.

IV. Conclusions

The Bakken Shale had high VOC mixing ratios similar to other locations with poor air quality such as the Denver-Julesburg Basin in Colorado and the Marcellus Shale in Pennsylvania. The amount of each VOC attributed to ONG sources was estimated in order to calculate the impacts that are directly related to ONG. The predominant source for the alkanes was ONG production with a range between 67 and 93% of these gases being emitted from ONG sources. Estimates of fluxes in the Bakken Shale were similar to those reported by multiple studies in Colorado and Pennsylvania. Calculated annual emission rates were higher in this study in comparison to those of Swarthout et al. (2013) and Petron et al. (2012), due to

many possible factors listed above. ONG emissions were estimated to contribute 20-40% of total OHR due to the large amount of reactive VOCs that are emitted through ONG processes compared to combustion processes. Alkanes were the largest contributor to ONG OHR at all three sites indicating that emissions of raw, unprocessed natural gas were primarily responsible for the observed ONG OHR.

The Bakken Shale has experienced a large increase in ONG production over the past 10 years. Quantifying emissions from both combustion sources and from development of ONG resources is important to understand the effects on regional air quality. A limited number of studies have analyzed VOC measurements in the proximity of the Bakken Shale despite the impact it has on federal lands and communities surrounding it. This study was the first to quantify source apportionment, provided the first preliminary emission flux estimate based on empirical data, and initiated steps towards estimating downwind impacts on air quality with OHR calculations.

V. Future Work

The estimated emission rates of calculated in this study were one order of magnitude higher than other studies, which implies that future work should be done to better understand the emission rates in the Bakken Shale UONG region. Specifically, studies to determine spatial and seasonal variability in emissions are needed. Unfortunately, this study was not able to obtain mixing ratios for methane, an important and potent greenhouse gas and the main component of natural gas. Future studies should measure methane and source apportionment and emission flux estimates should be repeated for this gas. Further research should be done to calculate the absolute amount of ozone formation expected from ONG emissions in the Bakken Shale region. While this study used the reaction rate between VOCs

and the hydroxyl radical as an estimate of potential ozone production, a more detailed investigation of absolute ozone production is needed to draw more concrete conclusions about air quality impacts. Atmospheric chemical models such as the community multiscale air quality model (CMAQ) should be used to understand the absolute impacts of ONG emissions on ozone formation. This information may play a large role in how cities implement policy and planning of transportation infrastructure which contribute to the levels of NO_x in an area which creates an environment primed for ozone production.

Acknowledgments:

I would like to acknowledge The National Park Service for sponsoring the Bakken Air Quality Study and collecting the whole air samples and the NOAA CIRES lab at University of Colorado at Boulder for analyzing the air samples and creating the rich dataset that I used in this research. In particular, Dr. Barkley Sive at the NPS and Dr. Yong Zhou at UC Boulder were integral in this work. I would like to thank Dr. Swarthout, my research advisor, for his expertise in this area and guidance throughout my research. I would like to thank Dr. Thaxton, my thesis reader and the Director of the Appalachian State University Environmental Science Program. Thanks to Donald Schelessman for providing data on the locations of ONG wells in the Bakken Shale used to create the study region map. Finally, I would like to express my gratitude to the students and staff of the Environmental Science Program for their continued support, encouragement, and friendship.

References

Atkinson, R. (2003), Kinetics of the gas-phase reactions of OH radicals with alkanes and cycloalkanes, Atmos. Chem. Phys., 3, 2233–2307. Atkinson, R., and J. Arey (2003), Atmospheric degradation of volatile organic compounds, Chem. Rev., 103, 4605–4638.

Atkinson, R., D. L. Baulch, R. A. Cox, R. F. Hampson, J. A. Kerr, M. J. Rossi, and J. Troe (1997), Evaluated kinetic, photochemical and heterogeneous data from atmospheric chemistry: Supplement V, J. Phys. Chem. Ref. Data, 26, 521–1011.

Atkinson, R., D. L. Baulch, R. A. Cox, J. N. Crowley, R. F. Hampson, R. G. Hynes, M. E. Jenken, M. J. Rossi, and J. Troe (2006), Evaluated kinetic and photochemical data for atmospheric chemistry. Volume II: Gas phase reactions of organic species, Atmos. Chem. Phys., 6, 3625–4055.

Baker, A. K., A. J. Beyersdorf, L.A. Doezema, A. Katzenstein, S. Meinardi, I. J. Simpson, D. R. Blake, R. F. Sherwood. "Measurements of nonmethane hydrocarbons in 28 United States cities." *Science Direct* 42 (2008): 170-82. Web. 22 Apr. 2017.

"Chemical composition of natural gas." *Union Gas*. N.p., 2006. Web. Apr. 2017.

Edwards, P. M., S.S. Brown, J. M. Roberts, R. Ahmadov, R. M. Banta, J. a. DeGouw, W. P. Dube, R. A. Field, J. H. Flynn, J. B. Gilman, M. Graus, D. Helmig, A. Koss, A. O. Langford, B. L. Lefer, B. M. Lerner, R. Shao-Meng Li, S. A. McKeen, S. M. Murphy, D. D. Parrish, C. J. Senff, J. Soltis, J. Stutz, C. Sweeney. "Seasonal cycle of O3 in the Uintah Basin, Utah and the Los Angeles Basin, California in 2013." *Nature* 514.7522 (2014): 351-54. Web. 23 Apr. 2017.

"Geology." *Bakken Shale Play*. Ked Interest LLC, 2009-2017. Web. 03 May 2017.

Gilman, J. B. "Source Signature of Volatile Organic Compounds from Oil and Natural Gas Operations in Northeastern Colorado." *Environmental Science & Technology* 47.3 (2013): 1297-305. Web. 2 Feb. 2017.

Holtzworth, George C. "Mixing depths, wind speeds and air pollution potential for selected locations in the United States." *Journal of Applied Meteorology* 6 (1967): 1039-044. Web. 20 Apr. 2017.

.

Katzenstein, A. S. "Extensive regional atmospheric hydrocarbon pollution in the southwestern United States." *Proceedings of the National Academy of Sciences* 100.21 (2003): 11975-1979. Web. 24 Apr. 2017.

Landrigan, P., C. B. Schechter, J. M. Lipton, M. C. Fahs, J. Schwartz. "Environmental

Pollutants and Disease in American Children: Estimates of Morbidity, Mortality, and Costs for Lead Poisoning, Asthma, Cancer, and Developmental Disabilities." *Children's Health Articles*. EPA, 2015. Web. May 2017.

"Petroleum Composition." *Petroleum Composition | what is the composition of petroleum*. N.p., 2013. Web. Apr. 2017.

Petron, G., A. Karion, C. Sweeney, B. R. Miller, S. A. Montzka, G. J. Frost, M. Trainer, P. Tans, A. Andrews, J Kofler, D. Helmig, D. Guenther, E. Dlugokencky, P. Lang, T. Newberger, S. Wolter, B. Hall, P. Novelli, A. Brewer, S. Conley, M. Hardesty, R. Banta, A. White, D. Noone, D. Wolfe, R. Schnell. "A new look at methane and nonmethane hydrocarbon emissions from oil and natural gas operations in the Colorado Denver-Julesburg Basin." *Journal of Geophysical Research* 119.11 (2014): 6836-852. Web. 24 Jan. 2017.

Petron, G., G. Frost, B. R. Miller, A. I. Hirsch, S. A. Montzka, A. Karion, M. Trainer, C. Sweeney, A. E. Andrews, L. Miller, J. Kofler, A. Bar-IIan, E. J. Dlugokencky, L. Patrick, C. T. Moore Jr., T. B. Ryerson, C. Siso, W. Kolodzey, P. M. Lang, T. Conway, P. Novelli, K. Masarie, B. Hall, D. Guenther, D. Kitzis, J. Miller, D. Welsh, D. Wolfe, W. Neff, P. Tans. "Hydrocarbon emissions characterization in the Colorado Front Range: A pilot study." *Journal of Geophysical Research* 117.D4 (2012): n. pag. Web. 3 Feb. 2017.

Prenni, A. J., D. E. Day, A R. Evanoski-Cole, B. C. Sivel, A. Hecobian, Y. Zhou, K. A. Gebhart, J. L. Hand, A. P. Sullivan, Y. Li, M. I. Schurman, Y. Desyaterik, W. C. Malm, J. L. Collett Jr., B. A. Schichtel. "Oil and gas impacts on air quality in federal lands in the Bakken region: an overview of the Bakken Air Quality Study and first results." *Atmospheric Chemistry and Physics* 16.3 (2016): 1401-416. Web. 12 Jan. 2017.

"Shale Research & Development." *Shale Research & Development | Department of Energy*. N.p., n.d. Web. 07 Apr. 2017.

Swarthout, R. F., R. S. Russo, Y. Zhous, A. H. Hart, B. C. Sive. "Volatile organic compound distributions during the NACHTT Campaign at the Boulder Atmospheric Observatory: Influence of urban and natural gas sources." *Journal of Geophysical Research: Atmospheres* 118.18 (2013): 10614-0637. Web. 20 Jan. 2017.

Swarthout, R. F., R. S. Russo, Y. Zhou, B. M. Miller, B. Mitchell, E. Horsman, E. Lipsky, D. C. McCabe, E Baum, B. C. Sive. "Impact of Marcellus Shale Natural Gas Development in Southwest Pennsylvania on Volatile Organic Compound Emissions and Regional Air Quality." *Environmental Science & Technology* 49.5 (2015): 3175-184. Web. 19 Jan. 2017.

US Environmental Information Administration. "Trends in U.S. Oil and Natural Gas Upstream Costs." (2016): 1-141. Web. Apr. 2017.

Webb, E., S. Bushkin-Bedient, A. Cheng, C. D. Kassotis, V. Balise, S. C. Nagel. "Developmental and reproductive effects of chemicals associated with unconventional oil and natural gas operations." *Pub Med* 29.4 (2014): 307-18. Web. Apr. 2017.